The Most Important Planes in Abdominal Ultrasound

(UA = upper abdomen; LA = lower abdomen)

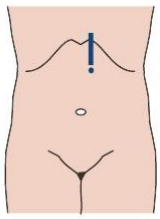 Sagittal upper abdomen left paramedian plane	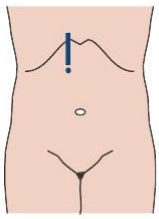 Sagittal upper abdomen right paramedian plane	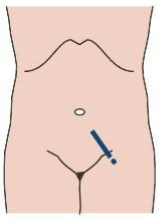 Oblique lower abdomen para-iliac plane
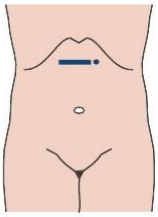 Transverse epigastric plane	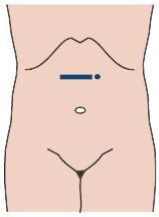 Transverse upper abdomen	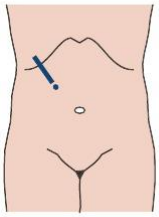 Oblique right upper abdomen
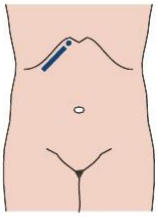 Right oblique subcostal plane (hepatic veins)	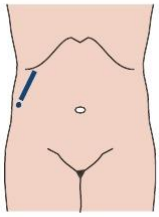 Longitudinal transhepatic plane	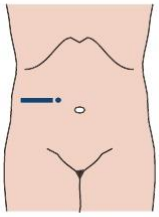 Transverse right midabdomen
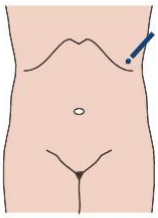 High plane of the left flank	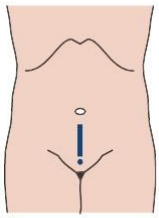 Median sagittal suprapubic plane	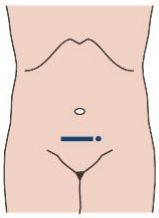 Transverse suprapubic plane

In this book, the point at the end of the position mark on the transducer corresponds to the right edge of the respective image. Think about which organs will be visualized in which respective imaging plane. To find the solutions, fold this page out and look on the back.

Standard Planes with Appropriate Transducer Position and Drawing Templates

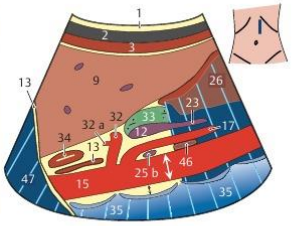

1. Sagittal upper abdomen, left paramedian plane (aorta)

Visualized organs and vessels:
Skin (1), subcutaneous fatty tissue (2), rectus abdominis muscle (3), lung (47), left lobe of the liver (9), stomach (26), pancreas (33), aorta (15), celiac trunk (32), left gastric artery (32a), superior mesenteric artery (17), superior mesenteric vein (23), diaphragm (13), five hypoechoic „eggs“: esophagus (34), crus of diaphragm (13), vertebral body (35) left renal vein (25b), horizontal part of the duodenum (46), confluence of the portal vein (12)

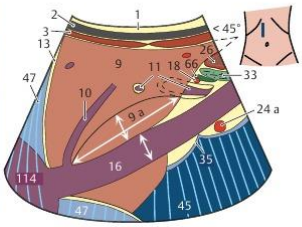

2. Sagittal upper abdomen, right paramedian plane (IVC)

Visualized organs and vessels:
Skin (1), subcutaneous fatty tissue (2), rectus abdominis muscle (3), lung (47), diaphragm (13), right atrium (114), stomach (26), pancreas (33), caudate lobe of the liver (9a), inferior vena cava (16), vertebral body (35), right renal artery (24a), branch of the portal vein (11) with accompanying bile duct branch (66) and branch of the hepatic artery (18), main vein (10) of the left lobe of the liver (9), acoustic shadow (45) behind the vertebral bodies (35)

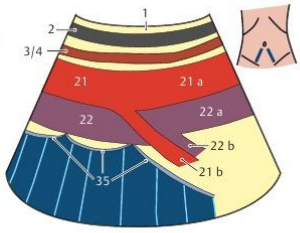

3. Oblique lower abdomen, para-iliac plane

Visualized organs and vessels:
Skin (1), subcutaneous fatty tissue (2), common iliac vein (22), external iliac vein (22a) and internal iliac vein (22b), common iliac artery (21), external iliac artery (21a) and internal iliac artery (21b), vertebral body (35), rectus abdominis muscle (3) or oblique muscles (4)

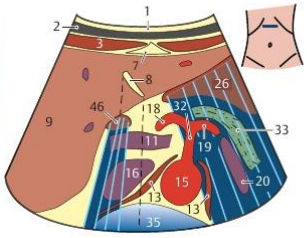

4. Transverse epigastric region (celiac trunk)

Visualized organs and vessels:
Skin (1), subcutaneous fatty tissue (2), rectus abdominis (3), ligamentum teres (7) and falciform ligament (8), liver (9), stomach (26), pancreas (33), duodenum (46), portal vein (11), hepatic artery (18), splenic artery (19) from the celiac trunk (32), splenic vein (20), aorta (15), inferior vena cava (16), diaphragm (13), vertebral body (35)

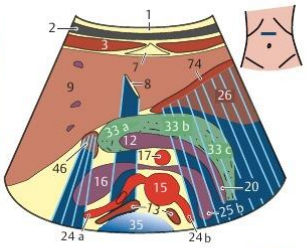

5. Transverse upper abdomen (renal vein crossing)

Visualized organs and vessels:
Skin (1), subcutaneous fatty tissue (2), rectus abdominis (3), ligamentum teres (7) and falciform ligament (8), liver (9), stomach (26), gastric wall (74), pancreas (33), duodenum (46), confluence of the portal vein (12), superior mesenteric artery (17), splenic vein (20), aorta (15), inferior vena cava (16), right renal artery (24a) and left renal artery (24b), diaphragm (13),vertebral body (35)

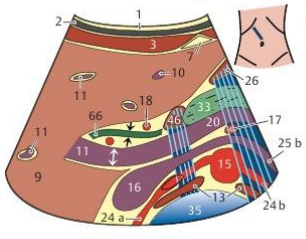

6. Oblique right upper abdomen (porta hepatis)

Visualized organs and vessels:
Skin (1), subcutaneous fatty tissue (2), rectus abdominis (3), ligamentum teres (7), liver (9), stomach (26), pancreas (33), duodenum (46), confluence of the portal vein (11), hepatic artery (18), common bile duct (66), splenic vein (20), aorta (15), right renal artery (24a) and left renal artery (24b), inferior vena cava (16), left renal vein (25b), diaphragm (13),vertebral body (35)

Standard Planes with Appropriate Transducer Position and Drawing Templates

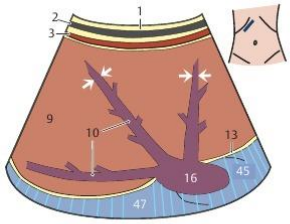

7. Right oblique subcostal plane (hepatic veins)

Visualized organs and vessels:
Skin (1), subcutaneous fatty tissue (2), rectus abdominis muscle (3), liver (9), hepatic veins (10), diaphragm (13), inferior vena cava (16), acoustic shadow (45) behind lung (47), measurement of width of hepatic veins (⇨) in the periphery of the liver < 6 mm

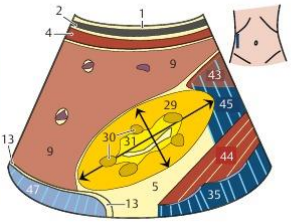

8. Longitudinal transhepatic plane showing right kidney

Visualized organs and vessels:
Skin (1), subcutaneous fatty tissue (2), oblique muscles (4), liver (9), hepatic veins (10), diaphragm (13), lung (47), renal parenchyma (29), medullary pyramids (30), renal caliceal system with renal pelvis (31), acoustic shadow (45) behind colon (43), connective tissue (5), psoas major muscle (44), vertebra (35), diaphragm (13)

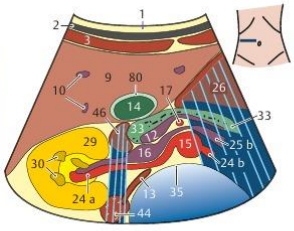

9. Transverse plane showing right kidney and IVC

Visualized organs and vessels:
Skin (1), subcutaneous fatty tissue (2), rectus abdominis muscle (3), liver (9), hepatic veins (10), gallbladder (14), gallbladder wall (80), stomach (26), duodenum (46), renal parenchyma (29), medullary pyramids (30), renal caliceal system with renal pelvis (31), psoas major muscle (44), vertebra (35), right renal artery (24 a), right rena lvein (25 a), inferior vena cava (16), aorta (15), confluence of the portal vein (12), pancreas (33), superior mesenteric artery (17)

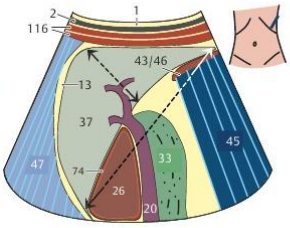

10. High plane of the left flank (spleen)

Visualized organs and vessels:
Skin (1), subcutaneous fatty tissue (2), intercostal muscles (116), lung (47), diaphragm (13), spleen (37), stomach (26), stomach wall (74), small bowel (46), colon (43), tail of the pancreas (33), splenic vein (20)

Caution:
Top edge of image = lateral
Bottom edge of image = medial

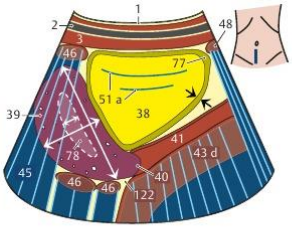

11. Median sagittal suprapubic plane (bladder and uterus)

Visualized organs and vessels:
Skin (1), subcutaneous fatty tissue (2), rectus abdominis muscle (3), acoustic shadow (45) behind the small bowel (46) and pubic bone (48), bladder (38), bladder wall (77), reverberation artifacts (51a), uterus (39), endometrium (78), vaginal portion (os) of cervix (40), vagina (41), rectum (43d), rectouterine pouch of Douglas (122)

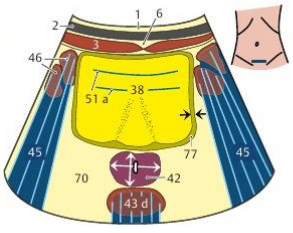

12. Transverse suprapubic plane (bladder and prostate gland)

Visualized organs and vessels:
Skin (1), subcutaneous fatty tissue (2), rectus abdominis muscle (3), linea alba (6), acoustic shadow (45) behind the small bowel (46), acoustic enhancement (70) behind the urinary bladder (38) with jets of urine from the ureteric orifices, bladder wall (77), reverberation artifacts (51a), prostate (42) or ovaries (91), rectum (43d)

Where Do I Find Which Chapter?

6 Tips for the Reader

Appendices

How can you best profit from this book?

How can you use this manual optimally?

As you work through the individual chapters, you can benefit from several methodical and didactic features.

Find it quickly ...

- Find a chapter: You will find the respective tab for each chapter on page 5.
- Find tough quiz questions for in-depth study.
- Find cross-referenced figures: The figures are numbered according to the page on which they appear. For example, Fig. 115.2 is on page 115.
- Find an explanatory figure or diagram supplementing the text. They are highlighted in the accompanying text in color and are almost always on the same page, eliminating the need to page through the book looking for them.
- Find numbered structures. Their reference numbers appear in bold in the accompanying text or on the back cover flap (the same number for each structure is used throughout the entire book).
- Find keywords on page 148 (or on pages 4-6).
- Find for each structure normal values and checklists. These are also provided on laminated, water-resistant, pocket-sized cards.

Why we call this book a "workbook"?

A unique feature of this book is that you can use each page as a quiz to test your knowledge. The diagrams contain reference numbers instead of labels. This means you can go through the material a second time and use any figure to test which structures you know and which you still have to learn. The quiz questions and drawing exercises have a similar purpose. In this way, you can become familiar with several efficient study methods that allow you to integrate new material into your long-term memory faster – even though this requires you to take a more active approach to learning. Not only do I wish you good luck with this course, I also hope you have fun doing it!

Matthias Hofer, MD, Associate Professor, MPH, MME, Summer 2020
Director of Education at the University Institute of Diagnostic, Interventional and Pediatric Radiology (DIPR)
Inselspital Bern, Bern University, Switzerland

What does the respective color coding mean in the diagrams?

- Tumors
- Arteries
- Veins
- Gallbladder wall
- Pancreas
- Bile
- Kidney
- Urine
- Connective tissue, fat
- Liver, thyroid gland
- Muscles
- Gastric lumen
- Air, bone
- Acoustic shadow
- Spleen, lymph nodes
- Prostate, uterus, ovary

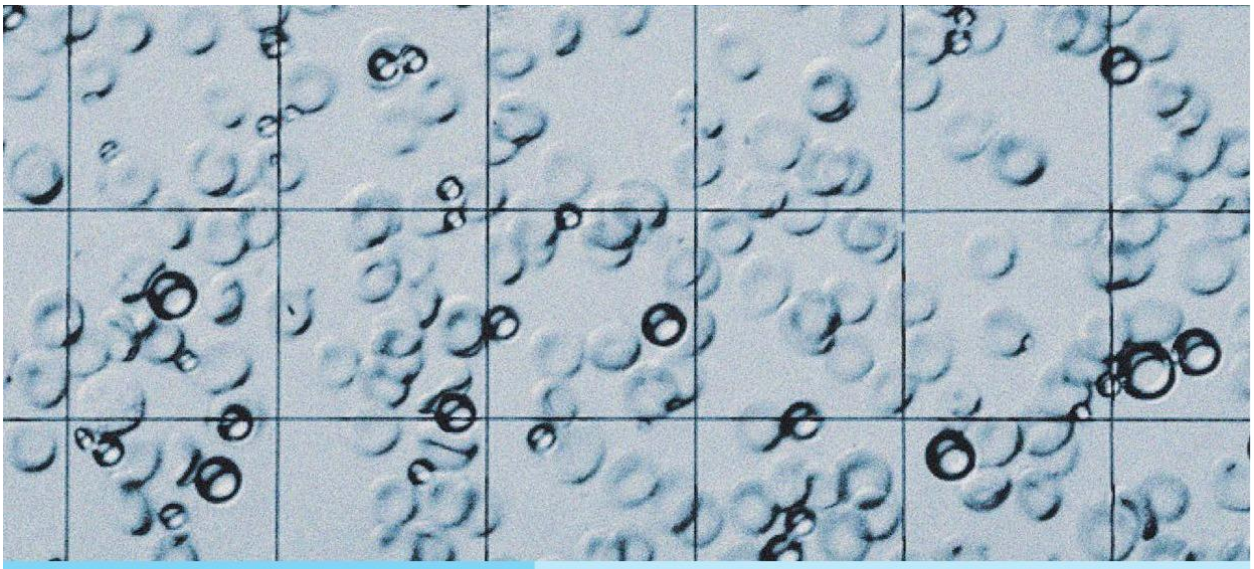

Introduction

Image Generation

Ultrasound images are generated not by X-rays but by sound waves that are sent by a transducer into the human body and reflected there. In abdominal ultrasound, the frequencies used generally are between 2.5 and 5.0 megahertz (MHz; see p. 11). The primary condition required for sound wave reflections is the presence of so-called "impedance mismatches." These occur at the interface between two tissue layers with different sound transmission properties (interfaces in Fig. 8.1). It is interesting to note that different soft tissues show only minor differences in the transmission speed of sound (Table 8.1).

Only air and bone are marked by massively different sound transmission in comparison with other human tissue. For this reason ultrasound units can be operated at a preselected medium frequency of approximately 1540 m/s without producing any major inaccuracies in the calculated origin ("depth") of the echo.

The processor computes the depth of origin of the echo from the time difference detected between emission of the sound impulse and return of the echo.

Echoes from tissue close to the transducer (**A**) arrive earlier (t_A) than echoes from deeper tissues (t_B, t_C in Fig. 8.1a). The mean frequency is strictly theoretical since the processor cannot know which type of tissue the sound waves traversed.

Sound Transmission in Human Tissue

Air	**331 m/s**	
Liver	1549 m/s	
Spleen	1566 m/s	m = 1540 m/s
Muscle	1568 m/s	
Bone	**3360 m/s**	

Table 8.1

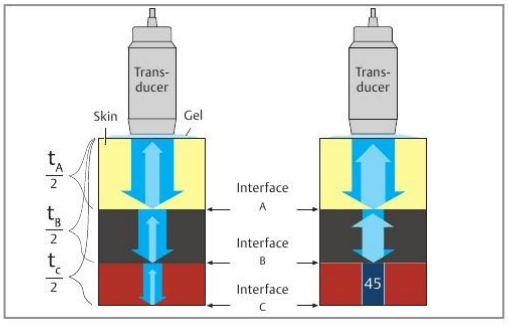

Fig. 8.1 a b

Which Component of the Sound Wave is Reflected?

Fig. 8.1a shows on the left three tissue blocks traversed by sound waves that differ only minimally in their transmission velocity (indicated by similar gray values). Each interface only reflects a small portion of the original sound waves (⇩) as echo (⇧). The right–hand diagram shows a larger impedance mismatch at the interface A between the different tissues (Fig. 8.1b). This increases the proportion of reflected sound waves (⇧) in comparison to the tissues shown on the left. However, what happens if the sound waves hit air in the stomach or a rib? This causes a so-called "total reflection," as illustrated at interface B in Fig. 8.2b: The transducer does not detect any residual sound waves deep to this structure from which it can generate an image. Instead, the total reflection creates an acoustic shadow (**45**).

Conclusion:

Intestinal or pulmonary air and bone are impenetrable by sound waves, precluding any imaging deep to these structures. The goal will later be to work around intestinal air or ribs by maneuvering the transducer. The pressure applied to the transducer against the abdominal wall (see p. 21) and the acoustic gel that displaces air between the surface of the transducer and the patient's skin (see p. 22) play a significant role.

From a "Snowstorm" to an Image ...

Do not get discouraged if at first you can only make out a blinding "snowstorm" on ultrasound images. You will be surprised how soon you will learn to recognize the ultrasound morphology of individual organs and vessels. Fig. 8.2 visualizes the gallbladder (**14**) as a black structure and shows two round polyps (**65**) within it. The surrounding gray "snowstorm" corresponds to the hepatic parenchyma (**9**) which is traversed by hepatic vessels (**10, 11**). How can you quickly work out which structures in the image appear bright and which are dark? The key lies in the concept of echogenicity (see p. 9).

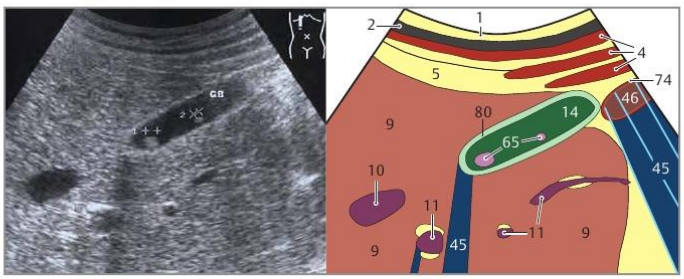

Fig. 8.2 a Gallbladder with polyps b

What Does the Term "Echogenicity" Mean?

Please use the following terms:	These fluids are anechoic (= black):
Hyperechoic (= bright)	pericardial or pleural effusion, ascites, cysts, blood, urine, bile, cerebrospinal fluid
Hypoechoic (= dark)	
Anechoic (= black)	

Tissues or organs with many intrinsic impedance mismatches produce many echoes and appear "hyperechoic" = bright. In contrast, tissue and organs with few impedance mismatches appear "hypoechoic" = dark. Consequently, homogeneous fluids without impedance mismatches (blood, urine, bile, cerebrospinal fluid, pericardial or pleural effusion, ascites, cyst secretion) appear "anechoic" = black. The number of impedance mismatches does not depend on the physical density (= mass per unit of volume). This is best illustrated with a fatty liver (**9**). On this noncontrasted CT scan (Fig. 9.1a), the parenchyma of a fatty liver appears darker (i.e., less dense) than hepatic vessels or normal liver (Fig. 9.1b).

This is due to the lesser density of fat in comparison with normal liver tissue. On ultrasound the fatty deposits produce more impedance mismatches (Fig. 9.1c) than in normal liver tissue (Fig. 9.1d). Consequently, a fatty liver appears more echogenic (brighter) on ultrasound despite its significantly lower physical density.

A common misunderstanding:
What do ultrasound examiners mean when they refer to a "dense liver"? Either they are not expressing themselves clearly or they have failed to grasp the fundamental principle of ultrasound imaging and how it differs from radiography. Ultrasound does not visualize physical tissue densities but differences in sound transmission (impedance mismatches) which are unrelated to density.

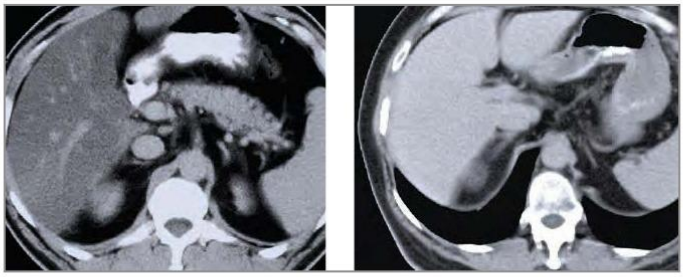

Fig. 9.1 a CT: Fatty liver b CT: Normal liver

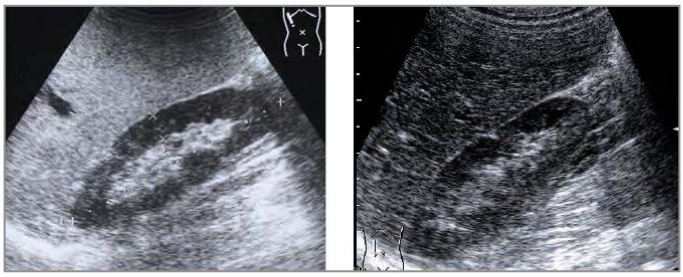

Fig. 9.1 c Ultrasound: Fatty liver d Ultrasound: Normal liver

Generation and Frequency Ranges of Sound Waves

Sound waves are generated by the reverse "piezoelectric effect." The pressure waves of an echo distort crystals, causing them to emit an electrical impulse. The reverse takes place during transmission. A transducer includes many such crystals. Depending on the impulse applied, they can produce sound waves of various frequencies specified in megahertz (MHz). A "3.75–MHz" transducer does not exclusively emit pressure waves (sound waves) at a frequency of 3.75 MHz. That is merely the specified median frequency (= "**center frequency**"). In fact, such a transducer may emit sound wave frequencies between, for example, 2 and 6 MHz. So-called "**multi frequency transducers**" have the additional capability to increase or decrease this center frequency and the surrounding bandwidth of transmitted sound frequencies. In thin patients or children, for instance, the bandwidth can be shifted (say 4–8 MHz with a center frequency of 6 MHz) to achieve better spatial resolution. However, this decreases the depth penetration of the sound waves.

In very obese patients, the use of lower frequencies (1–5 MHz with a center frequency of 2.5 MHz) can be appropriate to achieve the necessary penetration, but at the cost of lower resolution (see p. 11). Newer methods base their image generation on frequency shifts or harmonic frequencies of the echo in relation to the original ultrasound impulse (see p. 13).

Operating an Ultrasound Unit

Many controls on different ultrasound units are quite similar in function and arrangement regardless of the manufacturer. Therefore this section will look at the console of one unit supplied by Samsung (Fig. 10.1), which will then be used to introduce common technical terms.

Selection of Transducer and Preset

After you have switched on the unit (**A**) and it has booted, select the appropriate preset (**PS**) and the appropriate transducer for the respective examination and enter the current patient data (**PD**). You will usually select a linear array transducer (**L**) for evaluating the thyroid gland and the extremities but a convex array transducer (**C**) for abdominal examinations. The sector transducer (**E**) is used primarily in echocardiography, and the endovaginal transducer (**G**) is used for gynecologic examinations.

Selecting the Image Mode, Gain, and Focus

Usually you will begin with "normal" black and white or B-mode ultrasound (**B**), before later possibly switching to color-coded imaging (**C**). If you also wanted to obtain a flow profile from a blood vessel, you would then activate the Doppler mode (**D**) as well. This unit is equipped with control knobs that increase the respective signal (**gain**) of the active imaging mode when turned clockwise and reduce it when turned counterclockwise. The amplification (gain) can also be adjusted using the depth gain compensation feature (**G**). The transducer angle (**A**) must also be entered to determine flow velocities in Doppler mode. If you wish to display the change in a line of the image over time, switch to M-mode (**MM**). You can also set the specific depth range that is to have the best spatial resolution; here you use a toggle switch to set one or more focal zones (**FZ**) in your penetration depth. A few units also have a CW Doppler (**CW**) that measures frequency shifts (= flow speeds) not by means of depth gain compensation but as the summation of all speeds over an entire line of the image.

Magnification and Zoom Function

Especially with smaller target structures, you can significantly increase your detection of pathologic changes by magnifying the target organ (**Mag**) organ or zooming (**Z**) certain parts of the image. One common feature on almost all units is the position of the freeze or stop button (**St**) in the lower right corner of the console. This freezes the moving image. It is recommended to rest one finger of your left hand lightly on this button during the examination to minimize delay in capturing a desired image.

Size and Distance Measurements

After freezing (**St**) you can retrieve individual images from digital storage with the cine loop function: To do so, turn the trackball (**T**) to the left to 9:00 o'clock and go back image by image until you reach the desired one. Depending on the manufacturer and preset, up to eight simple measurements (**M**) can be performed one after the other on the frozen image. Use the trackball (**T**) and the set button (S) to define the beginning and end positions of your measured distances. It may be helpful to switch to double image mode (**2x**) for comparative measurements in different planes. Right next to this on most units is another button for switching back to single image mode (**1x**). More complex measurements such as volume measurements or flow indexes can be accessed with the measurement program (**MP**).

Helpful Extras

When you want to explain the imaging findings to the patient or a colleague, it is helpful to activate a pointer (**P**) which you can move across the frozen image with the trackball (**T**) to point out the findings you are explaining. If you really want to score points with your patients, install an additional monitor below the ceiling in their field of view. Well equipped units also offer automatic image optimization (**QS**), several hot keys for frequently used settings (P1-P3), and also several transducer sockets (**SP**) spare you the time and hassle of plugging and unplugging probes.

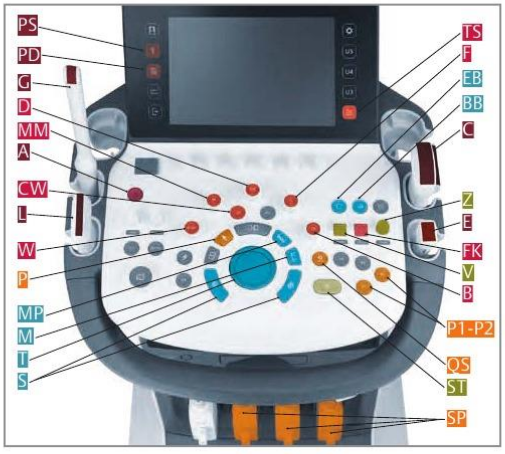

Fig. 10.1 Console and keypad

Selection of Ultrasound Units

In addition to large color Doppler units, ultrasound units with connections for several multi frequency transducers have proven especially useful in a hospital setting. Such mobile units are easily moved from the ultrasound suite to the ward or intensive care unit (Fig. 11.1).
The most important precaution when transporting the unit is to make sure that transducers are safely stowed so that dangling cables cannot become caught on doorknobs, gurneys, etc. A transducer that falls on the floor can easily represent a loss of €3000–7000 ($3300–7700) depending on the model. For the same reason, the transducer should never be left unattended on the patient's abdomen when the examination is interrupted, for instance by a telephone call. Stowing the transducer in the frame with the cable hanging avoids unnecessary kinking that can lead to broken conductors in the cable.

Types of Transducers

Of the many types of transducers, only the three most important ones will be discussed here (endovaginal transducers, see p. 103).
A linear array transducer or "parallel scanner" emits parallel sound waves into the tissue and produces a rectangular image (Fig. 11.2a). The width of the image and the number of scan lines remain constant at all tissue levels. Linear array transducers have the advantage of good near-field resolution and are primarily used with high frequencies (5.0–10.0 MHz or higher) for evaluating soft tissue and the thyroid gland. Their disadvantage is the large contact surface. This can lead to air gaps between skin and transducer when it is applied to a curved body contour (loss of acoustic coupling). Furthermore, acoustic shadowing (**45**) caused by ribs, lungs, or intestinal gas can greatly degrade image quality. Consequently, linear array transducers are rarely used for visualizing abdominal organs.

A **sector transducer** produces a fanlike image that is narrow near the transducer and increases in width with deeper penetration (Fig. 11.2b). This type of transducer has become established primarily in cardiology with lower frequencies (2.0–3.0 MHz) allowing deeper penetration. Due to the fanlike propagation of the sound waves, the heart can be well visualized through a small intercostal window without acoustic shadows from the ribs. The disadvantages of this type of transducer are their poor near-field resolution and decreasing line density in the far field with correspondingly decreasing resolution. Moreover, finding the desired imaging plane is difficult and takes some practice.

A curved or **convex array transducer** is a combination of the two types described above (Fig. 11.2c). The shape of the monitor image resembles a coffee filter and combines good near-field resolution with relatively good far-field resolution. The major advantage of the slightly curved contact surface is its ability to displace interfering intestinal air outside the imaging plane by applying increasing pressure (see p. 21). With this type of transducer, however, one has to accept decreasing resolution with increasing depth and, in certain locations, acoustic shadowing behind the ribs. This type is usually used in abdominal ultrasound with center frequencies from 2.5 MHz (in very obese patients) to 5.0 MHz (in slender patients).
The average frequency (center frequency) is usually 3.5–3.75 MHz. Memory aid: The higher the frequency, the better the resolution and the worse the penetration. The best way to remember this is to compare it to that loud music from your neighbor's apartment. Which tones best penetrate even thick walls? The basses. These lower frequencies travel farther (i.e., penetrate deeper), see page 9.

Fig. 11.1

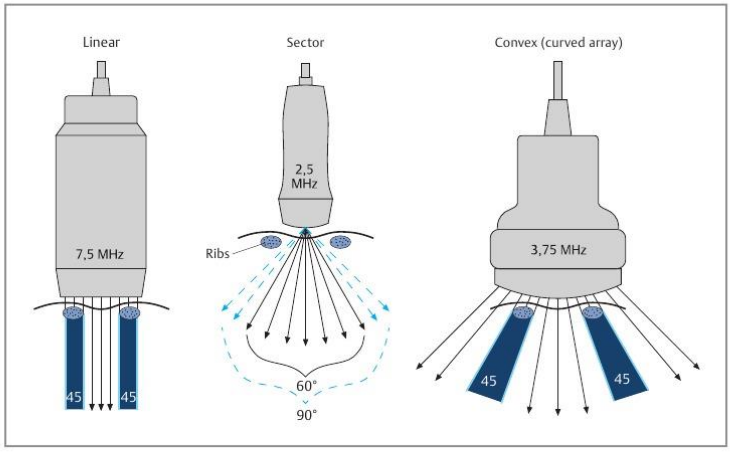

Fig. 11.2 a b c

12 New Techniques

Panoramic Imaging (SieScape®)

New high-performance image processors generate extensive ultrasound images from data acquired as the examiner moves the transducer slowly and continuously over the region of interest. With some practice, the examiner can produce impressive and undistorted images that allow distance measurements accurate to within 1–3% even on a curved body surface. Fig. 12.1 shows a sagittal scan with massive pleural effusion (**69**), compressive atelectasis of the lung (**47**), and, inferior to the liver (**9**), anechoic ascites (**68**) that appears to inundate the small bowel (**46**).

Fig. 12.2 impressively illustrates the position of the placenta (**94**) relative to the fetus. The high contrast resolution even allows evaluation of the interface between the fetal liver (**9**) and heart (**114**).

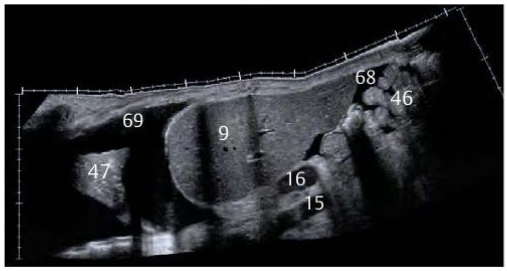

Fig. 12.1

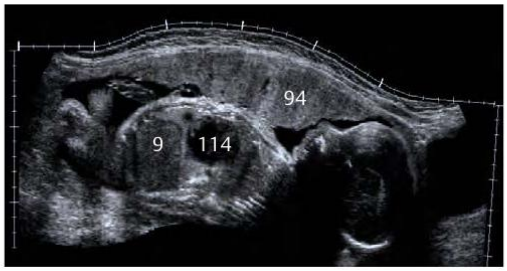

Fig. 12.2

(With kind permission of Drs. C.F. Dietrich and D. Becker, from Farbduplexsonographie des Abdomens, Schnetztor-Verlag, Konstanz, Germany)

3-D Visualization

Especially in obstetrics, the three-dimensional visualization of fetal facial features improves the diagnosis of malformations such as cleft lip and palate. This technique can now visualize the physiognomy of the fetal skull with amazing accuracy (Fig. 12.3).

Of course, conventional cross-sectional imaging techniques can also detect skeletal and other malformations, albeit less impressively and clearly than three-dimensional ultrasound.

Fig. 12.3

Clarify Vascular Enhancement Technology

This technique is based on an algorithm that is able to significantly reduce the blurring on B-mode scans resulting from partial volume or section thickness artifacts. Flow information from the power Doppler mode is used, which helps to improve the spatial resolution of vascular contours on the B-mode image.

The result is significantly improved visualization of findings such as the contours of hard and soft plaque in the carotid arteries (Fig. 12.4b) compared with the visualization achieved by the conventional technique shown in Fig. 12.4a. It also facilitates evaluation of peripheral vascular rarefaction in the liver as the lumens of the hepatic veins and portal venous branches are more clearly visualized in the hepatic parenchyma (Fig. 12.5).

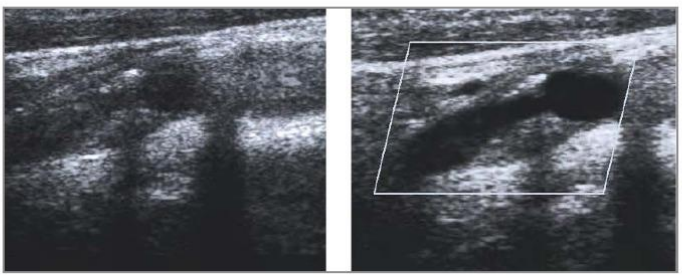

Fig. 12.4 a "Normal" image of the carotid artery ... b ... with Clarify

Fig. 12.5 Hepatic vessels

The material on the following five pages is not an absolute prerequisite for the first practice sessions and can be skipped. Beginners may prefer to move from here directly to the preparations for Lesson 1 (see p. 21). After some initial practice they should return to these pages to reinforce their fundamental understanding of ultrasound imaging.

Tissue Harmonic Imaging (THI): This technique does not use the fundamental frequency of the original ultrasound impulse but their harmonics, integer multiples of the fundamental frequency (for example 7.0 MHz for a fundamental frequency of 3.5 MHz). These harmonics increase with increasing penetration, but their amplitude (intensity) remains far less than that of the base signal. The advantage of these harmonics is that they hardly arise at all near the transducer, but only develop with increasing penetration depth (Fig. 13.1). Consequently, they are less affected by the major sources of scattered image noise, which occurs especially in the anterior abdominal wall. Why do harmonics develop only with increasing penetration depth? Ultrasound waves are distorted as they traverse tissues with varying acoustic properties. Their pressure waves compress and relax the tissue as they penetrate it. Compressed tissue increases the speed of sound. However, as the tissue relaxes, the speed decreases, causing the trough of the pressure wave to propagate more slowly. The resulting distortion of the wave form (Fig. 13.2) induces harmonics. This is a cumulative effect that increases with the depth of penetration. Consequently, the amplitudes of the harmonic frequencies initially increase with penetration depth until this increase is offset by general absorption (Fig. 13.1).

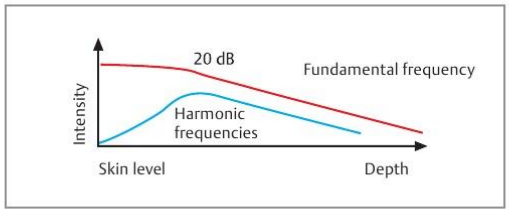

Fig. 13.1

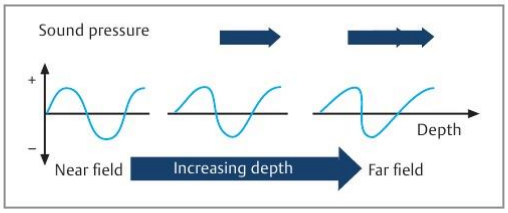

Fig. 13.2

Second Harmonic Imaging: This technique uses only the doubled frequency of the base signal for imaging. To avoid any overlapping of the range of the fundamental frequency (Fig. 13.3a) a narrowband signal must be used to distinguish the stronger components of the fundamental frequency from the weaker components of the harmonic (Fig. 13.3b). However, the narrower bandwidth of the signal leads to a slight reduction in contrast and spatial resolution. In spite of these shortcomings, this technique has markedly improved the detection of details (Fig. 13.4b) compared with conventional ultrasound imaging (Fig. 13.4a), especially in obese patients (whose abdominal wall produces excessive scattering).

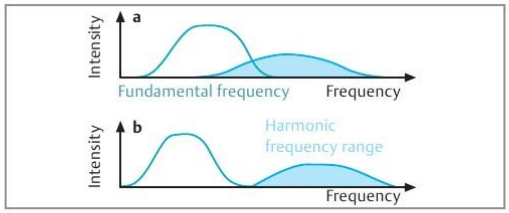

Fig. 13.3

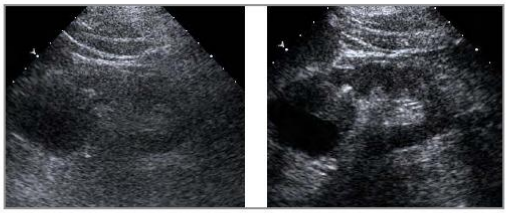

Fig. 13.4 a b

Phase Inversion Technique: A broadband technique has since become established that allows the use of dynamically optimized harmonic multiples of the transmitted frequency with a broader bandwidth (Fig. 14.1c, Ensemble® THI). With this technique, image optimization no longer depends on the narrow bandwidth of the fundamental frequency (Fig. 14.1a) to cleanly separate it from its harmonics (Fig. 14.1b). Two successive pulses are transmitted in such a way that the phase (upward excursion of the pressure = positive, downward excursion = negative) of the second pulse is inverted to the phase of the first pulse (Fig. 13.5).

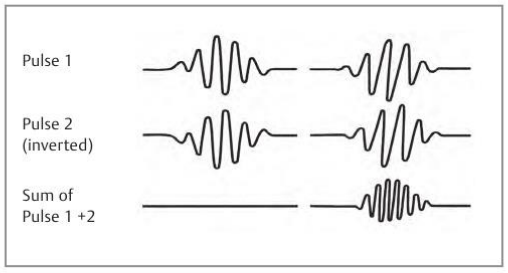

Fig. 13.5 a Linear b Nonlinear

If the echoes of both signals are added, the sum equals zero as long as the signal has not undergone any changes in the body. As a result, both fundamental frequency echoes are suppressed (Fig. 13.5a) whereas the second harmonic signal components are enhanced (Fig. 13.5b).

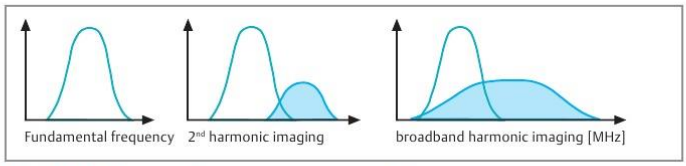

Fig. 14.1 a b c

Fig. 14.2 depicts a case showing acoustic shadowing (⇑⇑⇑) deep to intrarenal calcifications (**b**) that are undetectable by conventional imaging (**a**). In addition, the renal cyst (⇓) appears better demarcated and can be classified as benign with greater confidence.

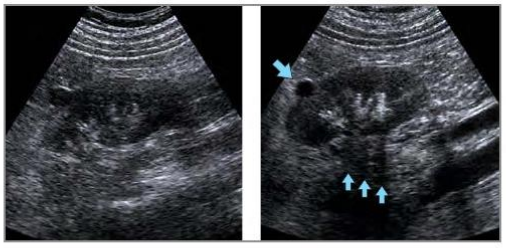

Fig. 14.2 a b

Contrast Enhancement

The echogenicity of blood and tissue can be enhanced with microbubbles with a diameter of 3–5 µm that pass through the capillaries and create more impedance mismatches within the blood stream (Fig. 14.3). So far, several contrast enhancement agents have been introduced and about 50 additional agents are under development. The contrast agent **Levovist**® consists of tiny air bubbles (✱) about 3 µm in diameter (95% < 10 µm), which are stabilized with a thin envelope of palmitic acid (Fig. 14.4). They are initially bound to galactose microparticles that dissolve in the blood and release the microbubbles. The dry powder can be mixed by the examiner in different concentrations. The suspension passes through the pulmonary circulation, but is only injectable for about 8 minutes after preparation. Hypergalactosemia is a contraindication. Measuring just a few millimeters, the microbubbles are comparable in size to erythrocytes (Fig. 14.5), which explains how they are able to pass through the capillaries.

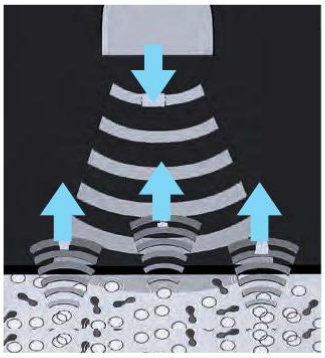

Fig. 14.3

Ultrasound impulses with low sound pressure make these microbubbles vibrate at what is known as a low "mechanical index" of 0.05–0.2. Contrast images are created using the nonlinear resonance frequency exclusively. Alternatively, one can use a higher mechanical index around 1.0–1.5 to cause the microbubbles to burst and emit a significantly stronger signal (although only during a single passage).This is known as the burst method.

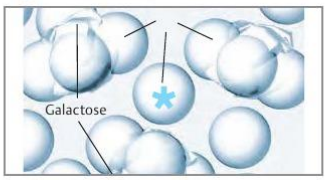

Fig. 14.4

The contrast agent **Sonovue**® consists of an aqueous solution of sulfur hexafluoride (SF6) stabilized by a phospholipid layer (Fig. 14.6). The median size of the bubbles is about 2.5 µm (90% < 8 µm) with an osmolality of 290 mOsmol/kg. One possible advantage of this contrast agent is that the suspension remains stable for over 6 hours, allowing it to be used for several applications. The best results are achieved in conjunction with the tissue harmonic imaging (THI) technique, referred to as "**contrast harmonic imaging (CHI)**." Frequently, the term **contrast-enhanced ultrasound (CEUS)** is also used.

A specific sound pressure causes the bubbles to vibrate and emit harmonic echoes. As a result, contrast harmonic imaging (Fig. 14.7b) can detect multiple liver metastases significantly better than noncontrasted imaging (Fig. 14.7a).

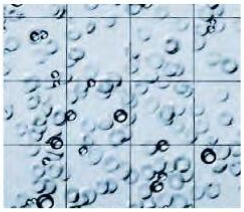

Fig. 14.5 Microbubbles

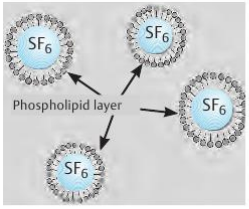

Fig. 14.6 Sonovue®

Fig. 14.7 a Noncontrasted b CEUS

Spatial Compounding (SonoCT®T)

There is another technique for suppressing artifacts. "Real-time compound imaging" does not scan an image line by line (Fig. 15.1a), instead it scans from different angles and merges this data into an image in real time (Fig. 15.1b). Up to nine different slices can be scanned, allowing more precise visualization of tissue information. This is illustrated here by the morphology of arteriosclerotic plaque in the carotid artery (⇩ in Fig. 15.2a) compared with conventional imaging (Fig. 15.2b).

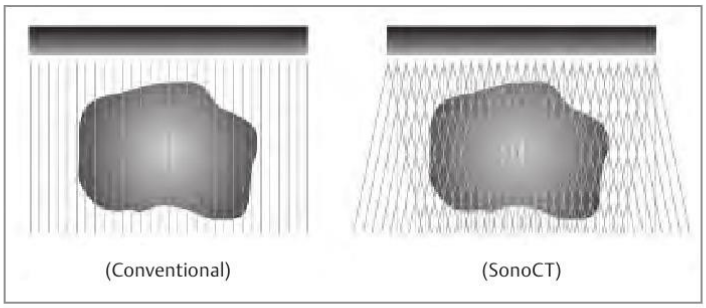

Fig. 15.1 a b

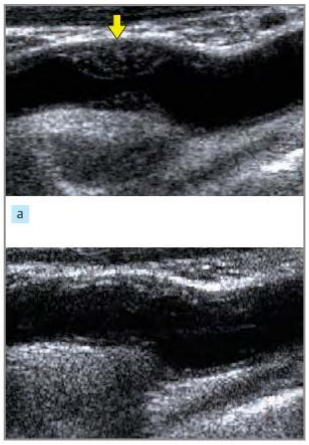

Fig. 15.2 b

This technique has exhibited obvious advantages in ultrasound imaging of the breast and musculoskeletal system. Fig. 15.3b shows improved visualization of an entire biopsy needle (⇘) in the breast parenchyma in comparison with conventional imaging (Fig. 15.3a), making it possible to advance the needle to the suspicious lesion with greater precision.

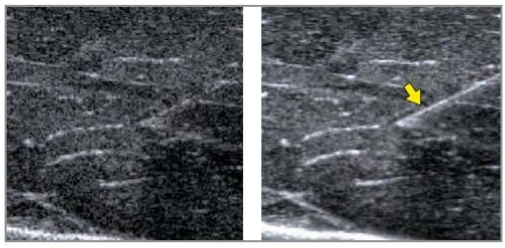

Fig. 15.3 a b

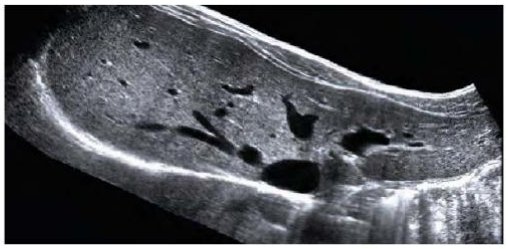

Fig. 15.4

The combination of SonoCT® scanning with tissue harmonic imaging (see p. 13) has shown promising results. It allows detailed visualization of hepatic lesions (Fig. 15.5) or fetal morphology in prenatal ultrasound screening (Fig. 15.6). The high performance computer systems now available can easily combine SieClear® or SonoCT® with three-dimensional (Fig. 15.7) and panoramic imaging techniques (Fig. 15.4). Here, almost the entire liver at the level of the hepatic venous system is visualized (see p. 52).

Fig. 15.5

Fig. 15.6

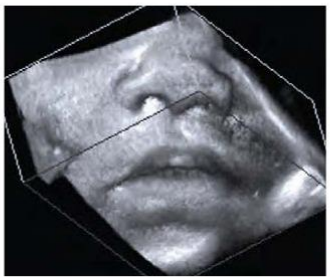

Fig. 15.7

Pulse Compression

This technique is derived from one originally developed for radar. Its main advantage is improved visualization of deep structures. It is not possible to increase penetration depth simply by increasing transmission power as this would produce undesirable thermal and mechanical effects. However, it is possible to increase the duration of the transmitted pulses and to modulate their frequency in a specific pattern ("chirp coding"). In this manner, the individual transmitted impulse has greater energy although its amplitude remains unchanged (Fig. 16.1a). The reflected echoes are then decoded by a chirp receiver filter and transformed back into shorter echoes of correspondingly higher amplitude (Fig. 16.1b).

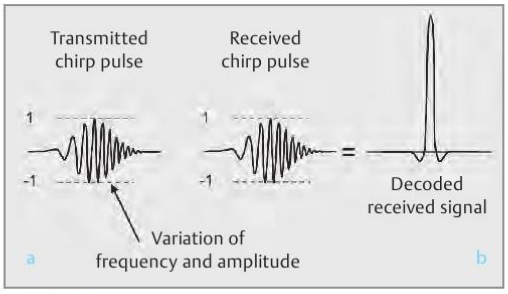

Fig. 16.1 Principle of pulse compression

The result is greater penetration depth with the degree of anatomic detail normally achieved only with lower frequencies and lower (and correspondingly worse) resolution. Fig. 16.2c shows a hypoechoic mass (**54**) deep to the thyroid gland (**81**) which would not have been visualized without pulse compression (Fig. 16.2a).

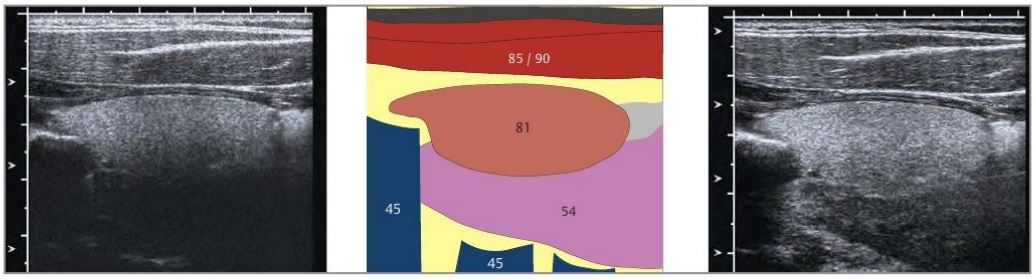

Fig. 16.2 a b c

Precision Upsampling

In conventional image processing techniques with high-frequency transducers, ultrasound echoes are scanned at a rate of only about 2–5 times the speed of the maximum frequency components of the echo (wide grid in Fig. 16.3a). Consequently, these echoes are only detected at a few points along their curve, and the monitor image really represents only an approximation of the actual echo signal (Fig. 16.4a). More complex reconstruction algorithms can record the duration and amplitude of the actual echo signal far more accurately (narrower grid in Fig. 16.3b). The result is that the structures of the radial tendon (⇧) shown here are visualized with significantly higher definition (Fig. 16.4b).

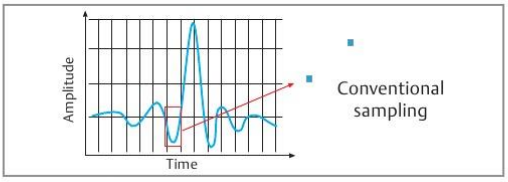

Fig. 16.3 a

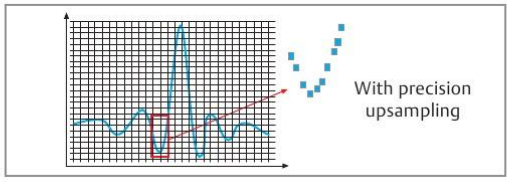

b

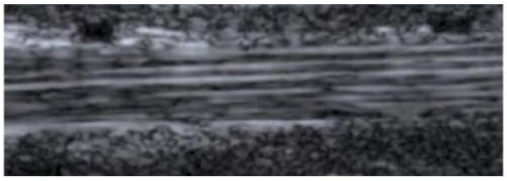

Fig. 16.4 a

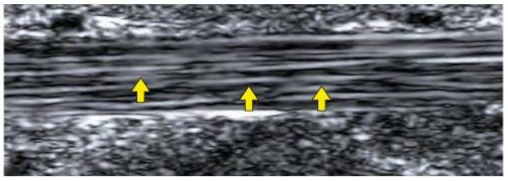

b